



Experimental investigation and optimization of the effects of manufacturing parameters on geometric tolerances in additive manufacturing of AlSi10Mg alloy

Yusuf Siyambaş¹ · Yakup Turgut²

Received: 17 March 2024 / Accepted: 9 July 2024 / Published online: 20 July 2024
© The Author(s) 2024

Abstract

While the quality of parts produced by additive manufacturing is generally evaluated by surface roughness, relative density, and mechanical properties, the issue of dimensional accuracy is not examined sufficiently. However, dimensional accuracy is very important for the final use and finishing of a product. Since the dimensional change mainly occurs due to shrinkage resulting from the heat energy applied during the sintering process, the effect of production parameters in the additive manufacturing method is quite large. To minimize shrinkage and increase dimensional accuracy, manufacturing parameters need to be optimized and meticulously examined. This study was aimed at determining the effects of manufacturing parameters on geometric tolerances in the production of parts using the additive manufacturing method. AlSi10Mg powder alloy and selective laser melting (SLM) technology were used in the additive manufacturing of this alloy in part production. Twelve different laser powers and scanning speeds, as well as fixed scanning range and layer thickness parameters, were used in production. In determining geometric tolerances, features such as hole diameter change, deviation from angularity, deviation from perpendicularity, deviation from flatness, and deviation from parallelism were taken into consideration. As a result of the study, deviation values increased in high and low laser power/scanning speed combinations. Minimum deviation amounts were obtained in the range of 250–310 laser power and 785–974 scanning speed, which are the middle values of the parameters used. The optimum values of different output responses have been obtained with different production parameters, but for the final use and quality control approval of the product, it is necessary to determine the input parameters at which all output responses are optimal. In this process, the gray relational analysis optimization method, which is one of the multi-criteria decision-making methods, was preferred. As a result of the optimization, the optimum manufacturing parameters for geometric tolerances were determined as the 290/911 laser power/scanning speed combination.

Keywords Additive manufacturing · AlSi10Mg alloy · Manufacturing parameters · Geometric tolerances · Gray relational analysis

1 Introduction

Additive manufacturing, also called rapid prototyping, has come to a position where different types of plastic and metallic materials are used with technological developments,

which has led to the development of different production methods [1]. Additive manufacturing is used in the manufacture of parts used in the medical, automobile, and aerospace industries [2]. Selective laser melting (SLM) is an advanced engineering application in metal-based additive manufacturing and is a preferred technology among LPBF methods. In this technology, metal powder is locally melted with a locally focused laser beam. The SLM method stands out with its ability to produce parts with complex structures, good surface quality, and excellent mechanical properties [3]. In addition, the SLM method is also suitable for mass production without the need for molds and production equipment, as in casting technology. Studies have also been carried out to produce materials that are superior in terms of

✉ Yusuf Siyambaş
yusuf.siyambas@erzincan.edu.tr

¹ Department of Machinery and Metal Technologies, Erzincan Binali Yıldırım University Vocational High School, Erzincan, Turkey

² Department of Manufacturing Engineering, Gazi University Faculty of Technology, Ankara, Turkey

microstructural and mechanical properties using the LPBF method [4–6]. The powder content and morphology used in metal-based additive manufacturing are very important in terms of product quality. In the literature, it has been stated that the homogeneity of the powder size contributes to obtaining a homogeneous layer thickness when spreading the powder on the manufacturing platform, and the fluidity of the powder has a significant effect on the spread of the powders on the manufacturing platform [7]. In addition, various powder shapes (irregular, angular, spherical, porous, rod-like, etc.) are also formed in powder production. It was reported that only spherical-shaped powder particles can provide high fluidity due to the minimum contact area of irregular powder particles with other powder particles [8]. Many materials have been used in additive manufacturing methods, and successful results have been obtained with a small number of material types. AlSi10Mg alloy is one of the materials where successful results are obtained in the process of reaching the final product in metal-based additive manufacturing [9]. AlSi10Mg alloy is the preferred material in many sectors due to its high casting ability, thermal conductivity, high specific strength, good electrical conductivity, and lightness [10, 11].

AlSi10Mg alloy parts produced in LPBF systems exhibit better mechanical properties than those produced by the traditional method (casting) [12]. However, there are important problems in terms of product geometry in the production of AlSi10Mg alloy parts. These problems arise from size, shape, direction, and location deviations on the part. If these deviations are too large, the usability of the part will be reduced. Therefore, in order for the produced part to function, these deviations must be as small as possible or within an acceptable value range. Geometric tolerances are especially important in the production of parts that form mechanisms that work with each other. Because parts that are not produced within the desired tolerance range will cause negative effects such as vibration and friction, which will reduce the usage time of the system. In this case, additional operations are required to reach the desired tolerance values, and additional operations cause loss of time and additional costs [13]. In this context, the subject is very important, and in-depth research needs to be done.

In order to improve the dimensional quality of parts produced by additive manufacturing, the variables that affect the physical process and cause defects must be well known [14]. In the studies, it has been stated that scanning speed, laser power, layer thickness, hatching distance, and overlap ratio are important parameters that affect the surface quality and dimensional accuracy of the parts produced with laser-based technologies [15–17]. In additive manufacturing, since the interaction between the energy given to the system and the material causes shrinkage, microstructure changes, and residual stresses in the final product, deviations in the

nominal geometry of the part are likely [18]. Changes in manufacturing parameters lead to changes in the cooling time and accompanying changes in the microstructure. This result affects the geometric accuracy due to the variability of the stresses in the parts. Researchers have conducted experimental and statistical studies to observe the impact of manufacturing parameters on dimensional accuracy. The effects of laser power, layer thickness, and scanning speed parameters on the relative density and Z direction shrinkage in the additive manufacturing of 316-L stainless steel material with the SLM method were investigated. It has been stated that the most effective parameter for the shrinkage rate is laser power, followed by scanning speed and layer thickness, respectively. It is emphasized that the size and shape accuracy of the produced parts in the Z direction can be improved by size compensation [19]. In another study, the effect of energy density on the dimensional deviation of 316-L stainless steel parts produced by the SLM method was investigated. As a result of the study, it was reported that dimensional deviation (height, diameter, and cylindricity) was greater at high-energy densities [20]. In another study, a theoretical model was proposed to estimate the accuracy obtained in horizontal measurements using the SLM method. It has been stated that the deviation in horizontal dimensions is the shrinkage that occurs during solidification due to the scanning mode and scanning range. To verify the model, parts were produced with Ti6Al4V material, and the created model was compared with experimental results. It has been reported that the model is in agreement with the experimental results and that thin-walled parts can be produced with a deviation of less than 20 μm using this model [21]. In another study, the effect of different scanning strategies on the dimensional accuracy of the internal structure in the production of Ti6Al4V powder material by the SLM method was examined. The dimensional accuracy of the internal structure gave better results in samples produced in the direction of scanning than in samples produced perpendicular to the scanning direction. Finite element analysis was used to verify this result, and it was said that the measurement accuracy increased with the uniform temperature distribution in the scanning direction. It was determined that the best results were obtained in the samples produced with the interlayer scanning angle change strategy [22]. In an experimental study, the dimensional accuracy and tolerance values of parts produced with three different additive manufacturing methods (LPBF, EBM, and LMD) were compared. It has been stated that different manufacturing methods may result in different dimensional accuracy at the same manufacturing parameters. Additionally, it was concluded that manufacturing parameters have an impact on dimensional accuracy and surface quality [18]. In another experimental study, the effects of manufacturing platform layout, temperatures, and part geometries on dimensional

change and residual stresses of parts produced with SLM were investigated. Part production was made in different geometries using Ti6Al4V powder material at fixed manufacturing parameters. It has been determined that the most effective parameters for residual stresses and dimensional changes are sudden cross-section changes, rapid cooling, and part height. It has been determined that the problems occurring in the parts can be reduced by 70% with additional coolants [23]. In another study, the effects of manufacturing parameters on part quality in additive manufacturing of AlSi10Mg alloy using the SLM method were investigated. It has been observed that while dimensional tolerances vary between large values such as 0.15–0.195 mm, the desired tolerance values can be obtained with higher hatching distances and scanning speeds [24]. In a study on additive manufacturing of Inconel 718 superalloy, the effect of layer thicknesses on dimensional accuracy was investigated. It has been stated that higher dimensional accuracy and density are achieved with lower layer thickness [15]. In another experimental study, the reason for the low accuracy in the Z direction in the additive manufacturing process was investigated. As a result of the study, it was concluded that the pressure loads applied to the layer stack may cause the layers to slide downwards. It has been reported that higher accuracy is achieved with appropriate-sized powder (23 μm) [25]. In another study, the effect of production parameters on geometric accuracy (flatness, circularity, cylindricity, and thickness) in parts produced by the FDM (Fused Deposition Modeling) method using ABS material was examined. As a result of the study, it was said that the filling ratio had a significant effect on geometric integrity [26]. Variable approaches have been used in tolerance analysis applied to non-traditional manufacturing processes such as metal-based additive manufacturing. In LPBF studies, dimensional accuracy is evaluated on final components [27, 28] or benchmark artifacts [29, 30]. The goal of experimental techniques based on geometric benchmark test artifacts, or GBTAs [31, 32], is to yield quantitative data on different geometric tolerance features. The properties of the GBTAs produced are used to characterize different dimensional and geometric tolerances [33–35]. The manufacturing parameter optimization and ranking that impact geometric tolerances come after the GBTA tests. The purpose of this information is to optimize these parameters for the real production process. Shahrain et al. varied 13 process parameters of a fused deposition modeling printer and, based on the experimental results for flatness and cylindricity, the parameters were ranked and optimized to meet the required geometric tolerance of subsequent prints [36]. In order to determine the features of the geometric tolerances needed for the additive manufacturing process, several researchers have reported their experimental findings utilizing geometric benchmark test artifacts (GBTA) [37, 38]. In multi-response systems, the parameters that give

the optimum result may vary. In this regard, it becomes difficult to determine the optimum parameters. Multi-criteria decision-making (MCDM) approaches are used to solve such problems [39]. One of these approaches is the gray relational analysis (GRA) method. The GRA method has been widely used to solve multi-output problems with high accuracy. Research shows that the GRA method can be used to find the most ideal alternative quickly and easily [40–42].

When the studies are examined, it is seen that the effects of manufacturing parameters on product quality and dimensional accuracy in additive manufacturing processes are investigated. In order to determine the features of the geometric tolerances needed for the additive manufacturing process, several researchers have reported their experimental findings utilizing geometric benchmark test artifacts (GBTA). However, since geometric tolerances are one of the most important factors affecting the usability of metal-based parts, further studies should be carried out to determine the optimum parameters. In this study, in addition to the literature, we focused on the effect of laser power and scanning speed on geometric tolerances in the additive manufacturing of AlSi10Mg alloy and evaluated its performance properties together. In addition, manufacturing parameters are simultaneously optimized for performance features such as hole diameter change (DC), deviation from angularity (AD), deviation from perpendicularity (PD), deviation from flatness (FD), and deviation from parallelism (PAD). In this context, it is aimed at determining the manufacturing parameters that provide the best alternative using the gray relational analysis method.

2 Material and method

2.1 Production of parts and determination of tolerance values

The parts used in this study were produced according to the manufacturing parameters given in Table 1. Firstly, the ideal volumetric energy density for additive manufacturing of AlSi10Mg alloy was investigated in determining the fabrication parameters. In this context, preliminary studies on mechanical properties and surface roughness were carried out, and the ideal volumetric energy density for this alloy was determined to be 55.82 J/mm³ [43]. It has been stated in the literature that the main parameters affecting the dimensional accuracy of metal-based additive manufacturing methods are laser power, scanning speed, print orientation, and build direction [44]. Since the study focuses on volumetric energy density, laser power and scanning speed were used as variable parameters. Then, parts were produced at this volumetric energy density using different laser power and scanning

Table 1 Experimental design used in the production of parts

Part number	Laser power (W)	Scanning speed (mm/s)	Hatching distance (mm)	Layer thickness (mm)	Volumetric energy density (J/mm ³)
1	390	1225			
2	370	1162			
3	350	1100			
4	330	1037			
5	310	974			
6	290	911	0.19	0.03	55.82
7	270	848			
8	250	785			
9	230	722			
10	210	660			
11	190	597			
12	170	534			

Table 2 Chemical composition of AlSi10Mg alloy [45]

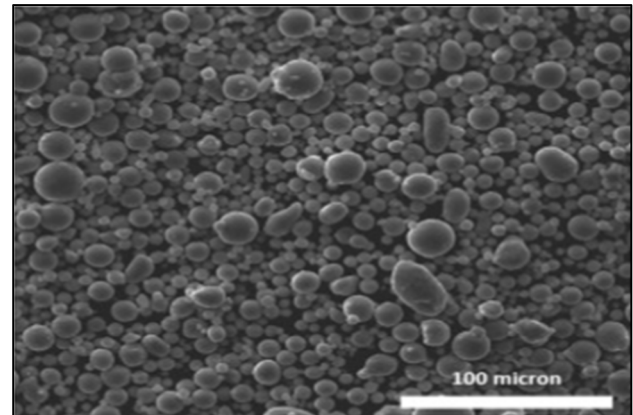
Element	C	Cu	Fe	Mg	Mn	Ni	O	Pb	Si	Ti	Zn	Sn	Al
Weight (%)	<0.005	<0.03	0.13	0.38	<0.03	<0.03	0.114	<0.03	10.3	<0.03	<0.03	<0.03	Bal

Table 3 Powder size distribution of AlSi10Mg alloy according to ASTM B822 [45]

Size (μm)	D10	D50	D90	<5
Min	5	26	45	-
Max	15	36	55	10%

speeds, a fixed hatching distance, layer thickness, and a 67° variable angle scanning strategy. In addition, 0.1 mm laser beam focus diameter, 1 laser, 30 °C manufacturing platform temperature, and 25–35 °C manufacturing room temperature were used in the production of the parts. The AlSi10Mg alloy produced by the gas atomization method was used in the production of its parts. The chemical composition of the AlSi10Mg alloy is presented in Table 2. The size distribution of the powder material used in part production is in the range of 5–55 μm, and its details are given in Table 3. The morphology of this powder alloy was examined by scanning electron microscopy, and it was determined that it had a spherical morphology (Fig. 1). A Concept Laser-M2 CUSING brand printer with an SLM system was used in the production of the parts. The printer has a wavelength of 1070 nm and a 400W Ytterbium (Yb) fiber laser. The manufacturing process was carried out in an argon atmosphere to prevent oxidation.

Prismatic parts were produced to ASME 14.5 standards to investigate the effect of scanning speed and laser

**Fig. 1** Morphology of AlSi10Mg alloy

power on geometric tolerances [46]. The dimensions of the produced part and the location of the tolerances on the part are given in Fig. 2. The flow chart followed in the experimental study is shown in Fig. 3. In addition, detailed explanations of geometric tolerances are given in Fig. 4. Diameter measurement change, deviation from angularity, perpendicularity, flatness, and parallelism were used in the investigation of geometric tolerances. Hole number 3 was taken into consideration for diameter change, and angle number 1 was taken into consideration for deviation from angularity.

Geometric tolerance values were obtained using a Hexagon brand Coordinate Measuring Machine (CMM)

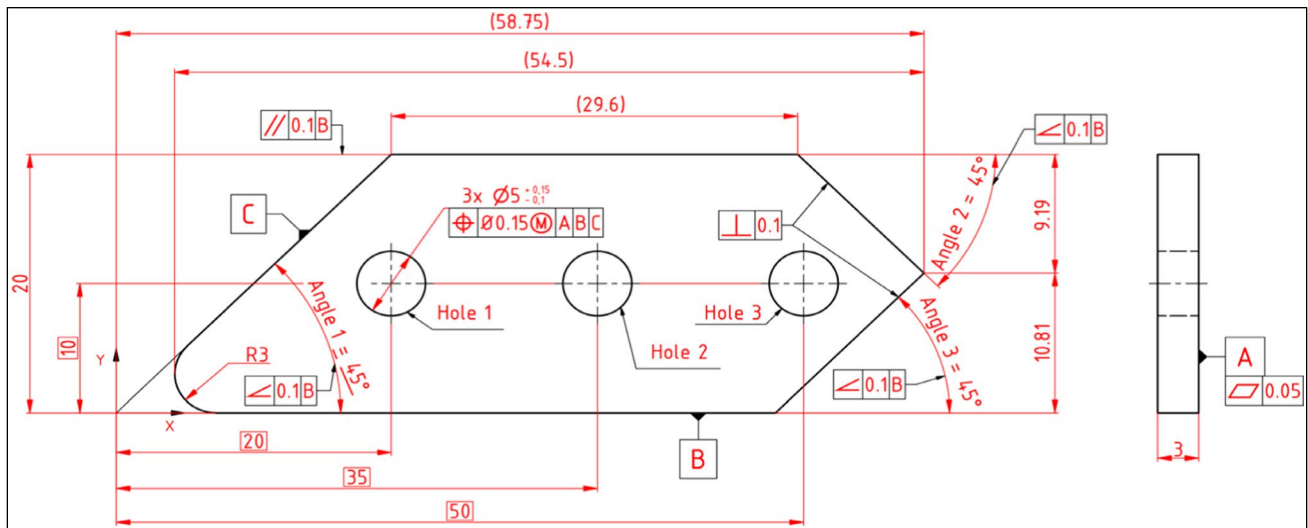


Fig. 2 Technical drawing of the part produced for geometric tolerances

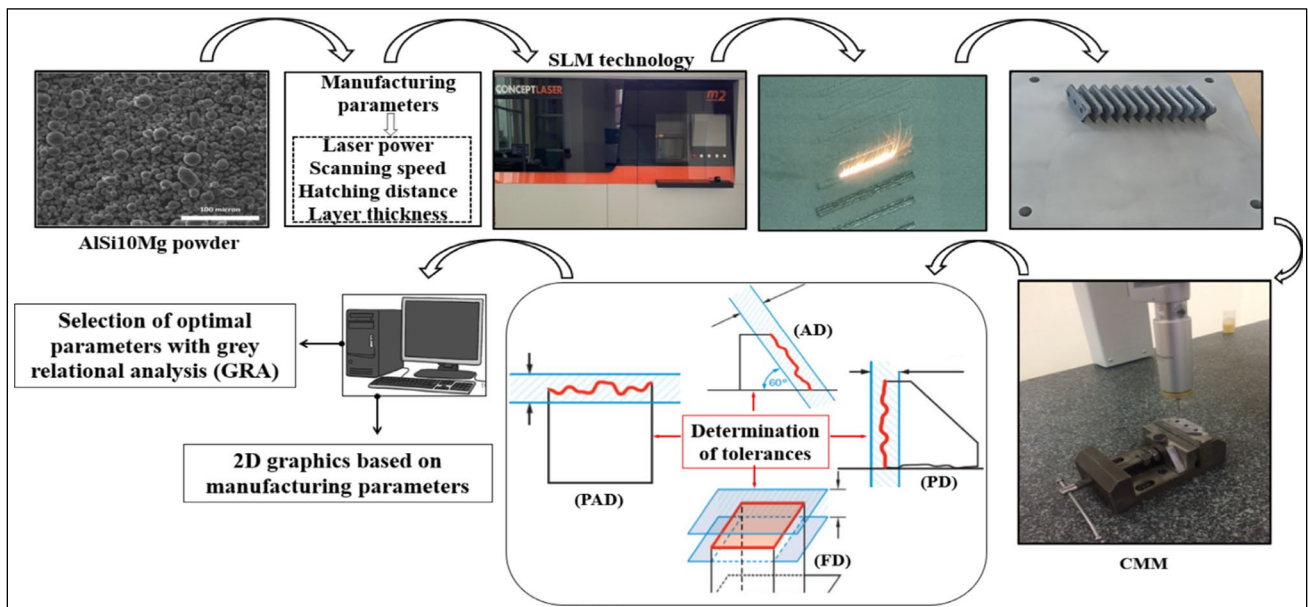


Fig. 3 Flowchart used in the research experiment

device with a 2-mm diameter probe. The measurement accuracy of this device is 1 μm. Three measurements were taken for the investigated features, and experimental results were obtained by calculating the average of these measurements. Figure 5 shows the visual of measuring part 2 with the CMM device. Hole images on the parts were obtained with an AM413ZT Polarizing Digital Microscope at 16× magnification. Deviation values were calculated to observe the change of measured values compared to nominal values (Eq. 1).

$$Deviation\ value = |nominal\ value - measured\ value| \quad (1)$$

2.2 Gray relational analysis

The optimal combination of parameters is very important in obtaining the required result with the minimum use of resources. The parameter set that is appropriate for a particular output may not be suitable for other outputs. In this regard, MCDM methods are needed to determine the optimum parameter set. Among MCDM methods, GRA is


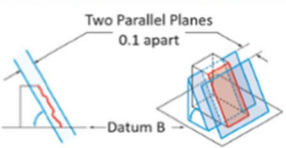
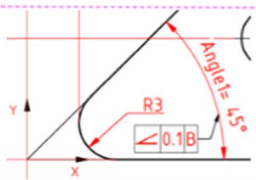
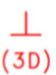
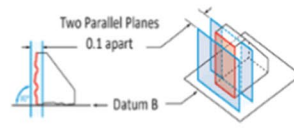
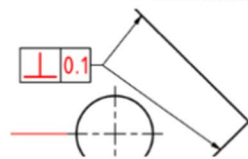

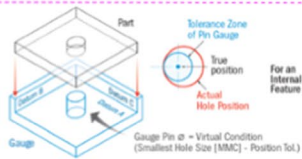
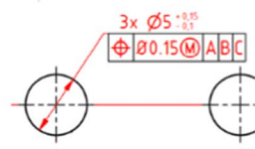
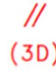
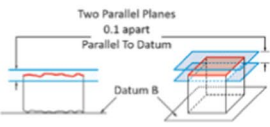
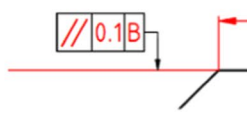

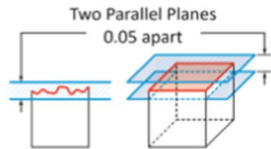
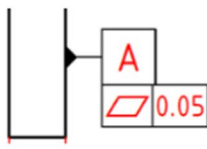
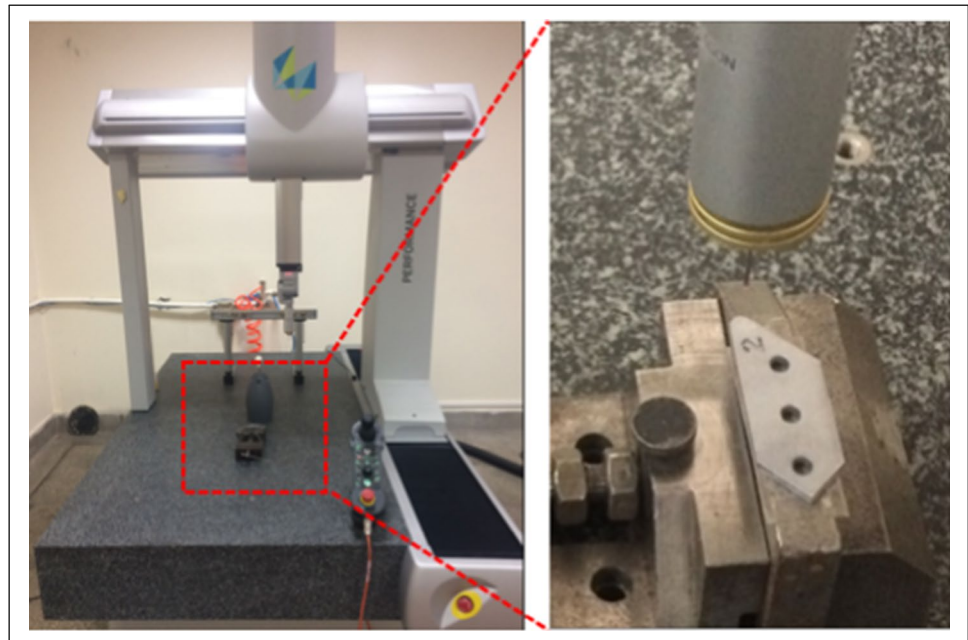
Symbol & control	Description of tolerance zone	Tolerance zone	Representation in technical drawing	Description
	The tolerance zone spanning a plane is limited to two parallel planes spaced 0.1 apart at the specified angle inclination with respect to the reference plane.			The compensated plane A must lie between two parallel planes spaced 0.1 apart at 45° inclination with respect to the reference axis.
	When tolerance is specified in one direction only, the tolerance zone spanned in a plane is limited to two parallel lines spaced 0.1 apart perpendicular to the reference plane.			The 2 planes indicated by the arrow must lie between two parallel planes spaced 0.1 apart.
	3 When the Ø symbol is placed in front of the tolerance value of the hole, the tolerance zone is limited to a 0.15 diameter cylinder whose axis is located at the theoretical exact location.			The axis of the bore must lie in a 0.15 diameter cylinder at its theoretical exact location in reference planes A, B, and C.
	The tolerance zone is limited to two 0.1 spaced planes parallel to the reference plane.			The tolerant surface must lie between two planes parallel to the reference plane B in the range 0.1.
	The tolerance zone is limited to two parallel planes spaced 0.05 apart.			The surface must lie between two parallel planes spaced 0.05 apart.

Fig. 4 Detailing of geometric tolerances (<https://www.gdandtbasics.com/gdt-symbols>)

Fig. 5 Preparation for measurement of part 2 with CMM



widely used in solving MCDM problems. The aim of this study is to determine the manufacturing parameters that give the best alternative in terms of geometric tolerances using the GRA method. In the GRA method, the deviation values first obtained are normalized. The purpose of normalization is to eliminate variability and bring deviation values into a comparable range of 0–1. The most important factor to consider in normalization is which approach will be used. In this study, since the deviation values were desired to be small in terms of product quality, the lower the better approach was used in the normalization process. Deviation values were obtained by subtracting the normalized values from 1. Gray relational coefficients (GRC) were then calculated. Finally, gray relational degrees (GRG) were created by averaging the gray relational coefficient. The equations used in making the calculations are given below [47–49].

The normalization process can be carried out in three different ways according to benefit, cost, and optimal situations (Eqs. 2–4).

In the case of the larger the better, the original sequence can be normalized as follows:

$$x_i(k) = \frac{x_i^0(k) - \min x_i^0(k)}{\max x_i^0 - \min x_i^0(k)} \tag{2}$$

In the case of the smaller the better, the original sequence can be normalized as follows:

$$x_i(k) = \frac{\max x_i^0(k) - x_i^0(k)}{\max x_i^0 - \min x_i^0(k)} \tag{3}$$

In the case of the nominal the better, the original sequence can be normalized as follows:

$$x_i(k) = 1 - \frac{x_i^0(k) - x^0}{\max x_i^0 - x^0} \tag{4}$$

$x_i^0(k)$ original value at i series k . row, $x_i(k)$ after normalization value at i series k . row, $\min x_i^0(k)$ is the minimum value at i series, $\max x_i^0(k)$ is the maximum value at i series, and x^0 denotes the desired ideal value. k denotes the k . row in the series at n length. $\varepsilon(x_0(k), x_i(k))$ is the gray relational coefficient at k . point, and is given in Eqs. 5–8.

$$\varepsilon(x_0(k), x_i(k)) = \frac{\Delta_{\min} + \xi \Delta_{\max}}{\Delta_{0i}(k) + \xi \Delta_{\max}} \tag{5}$$

$$\Delta_{0i}(k) = |x_0(k) - x_j(k)| \tag{6}$$

$$\Delta_{\min} = \min_j \min_k |x_0(k) - x_j(k)| \tag{7}$$

$$\Delta_{\max} = \max_j \max_k |x_0(k) - x_j(k)| \tag{8}$$

$\xi \in (0, 1)$. $j = 1, 2, \dots, m$; $k = 1, 2, \dots, n$. ξ function arranges the difference between Δ_{0i} and Δ_{\max} . Studies show the ξ function does not affect the post-gray relation degree order [50]. In the last step, the gray relational degree is calculated by Eq. 9.

$$\gamma(x_0, x_i) = \frac{1}{n} \sum_{k=1}^n \varepsilon(x_0(k), x_i(k)) \tag{9}$$

$\gamma(x_0, x_i)$ is a measure of geometric similarity between the x_i and x_0 reference series in a gray system. The size of the gray relational degree shows a strong relationship between x_i and x_0 . If the series being compared are the same, the gray relationship degree is 1. The gray relational degree demonstrates how the compared series is similar to the reference series.

3 Result and discussion

In this study, AlSi10Mg alloy parts were produced by the SLM method using different laser power and scanning speed parameters. The effect of parameters on geometric tolerances on the produced parts was investigated. The results obtained from the experimental study are given in Table 4.

When the results were examined, the diameter value was found to be smaller than the nominal value. The angularity and perpendicularity values were obtained higher than the nominal value. Deviation values were calculated by subtracting the obtained results from the nominal values (Table 5). The calculated deviation values were evaluated separately by creating graphs of diameter change, deviation from angularity, deviation from perpendicularity, deviation from flatness, and deviation from parallelism, depending on the manufacturing parameters.

3.1 Evaluation of diameter change

The variation of diameter change depending on laser power and scanning speed parameters in additive manufacturing of AlSi10Mg alloy is given in Fig. 6. For hole number 3, the minimum amount of deviation from the diameter was obtained at the 290/911 laser power/scanning speed combination. This value is the middle value of the manufacturing parameters. As this value increases and decreases, the amount of deviation from the nominal value increases.

When the hole diameter change is evaluated in terms of the specified tolerance range, hole size number 3 was obtained within the tolerance value range in the 6th part. In the SLM method, the powder material is heated locally and rapidly above its melting temperature and then allowed to solidify and cool to form a dense geometry.

Table 4 Results obtained depending on manufacturing parameters

Manufacturing parameters			Performance characteristics and numerical values obtained				
Part no	Laser power (W)	Scanning speed (mm/s)	Diameter change (DC) (mm)	Deviation from angularity (AD) (°)	Deviation from perpendicularity (PD) (°)	Deviation from flatness (FD) (mm)	Deviation from parallelism (PAD) (mm)
1	390	1225	4.708	45.506	91.07	0.023	0.059
2	370	1162	4.633	45.636	90.85	0.020	0.045
3	350	1100	4.716	45.709	91.08	0.037	0.026
4	330	1037	4.749	45.552	90.54	0.006	0.024
5	310	974	4.751	45.370	90.08	0.005	0.017
6	290	911	4.904	45.017	90.59	0.003	0.012
7	270	848	4.793	45.544	91.15	0.010	0.004
8	250	785	4.769	45.432	90.10	0.013	0.021
9	230	722	4.771	45.618	91.14	0.015	0.031
10	210	660	4.888	45.487	91.32	0.018	0.045
11	190	597	4.770	45.769	90.83	0.025	0.045
12	170	534	4.778	45.649	90.97	0.029	0.067

Thus, internal stresses and distortions occur in the parts produced due to the nature of the process. One of the most common approaches used to reduce these negative effects on the part is optimizing manufacturing parameters [51]. The main parameters affecting the dimensional accuracy of metal-based additive manufacturing methods are laser power and scanning speed [44]. Studies have shown that accuracy tends to decrease as laser power increases and that dimensional accuracy can be increased to some extent if high scanning speeds are used [21, 52]. The smaller diameter variation at intermediate values of the manufacturing parameter can be attributed to the formation

of small melt pools, leading to lower shrinkage effects and therefore higher dimensional accuracy. Also, the hole images taken from the parts are given in Fig. 7.

3.2 Evaluation of deviation from angularity and perpendicularity

The variation of angularity and perpendicularity deviation depending on laser power and scanning speed parameters in the additive manufacturing of AISi10Mg alloy is given in Fig. 8. When the angularity deviation graph given in Fig. 8a is examined, the lowest amount of deviation was obtained

Table 5 Deviation and normalized values

Part no	Deviation values					Normalized values				
	DC	AD	PD	FD	PAD	DC	AD	PD	FD	PAD
1	0.292	0.506	1.07	0.023	0.059	0.2768	0.3497	0.2016	0.4118	0.1270
2	0.367	0.636	0.85	0.02	0.045	0.0000	0.1769	0.3790	0.5000	0.3492
3	0.284	0.709	1.08	0.037	0.026	0.3063	0.0798	0.1935	0.0000	0.6508
4	0.251	0.552	0.54	0.006	0.024	0.4280	0.2886	0.6290	0.9118	0.6825
5	0.249	0.37	0.08	0.005	0.017	0.4354	0.5306	1.0000	0.9412	0.7937
6	0.096	0.017	0.59	0.003	0.012	1.0000	1.0000	0.5887	1.0000	0.8730
7	0.207	0.544	1.15	0.010	0.004	0.5904	0.2992	0.1371	0.7941	1.0000
8	0.231	0.432	0.10	0.013	0.021	0.5018	0.4481	0.9839	0.7059	0.7302
9	0.229	0.618	1.14	0.015	0.031	0.5092	0.2008	0.1452	0.6471	0.5714
10	0.112	0.487	1.32	0.018	0.045	0.9410	0.3750	0.0000	0.5588	0.3492
11	0.230	0.769	0.83	0.025	0.045	0.5055	0.0000	0.3952	0.3529	0.3492
12	0.222	0.649	0.97	0.029	0.067	0.5351	0.1596	0.2823	0.2353	0.0000
Average	0.23	0.52	0.81	0.02	0.03					
Standart dev	0.0731	0.1962	0.4058	0.0104	0.0193					

Fig. 6 Diameter change according to manufacturing parameters

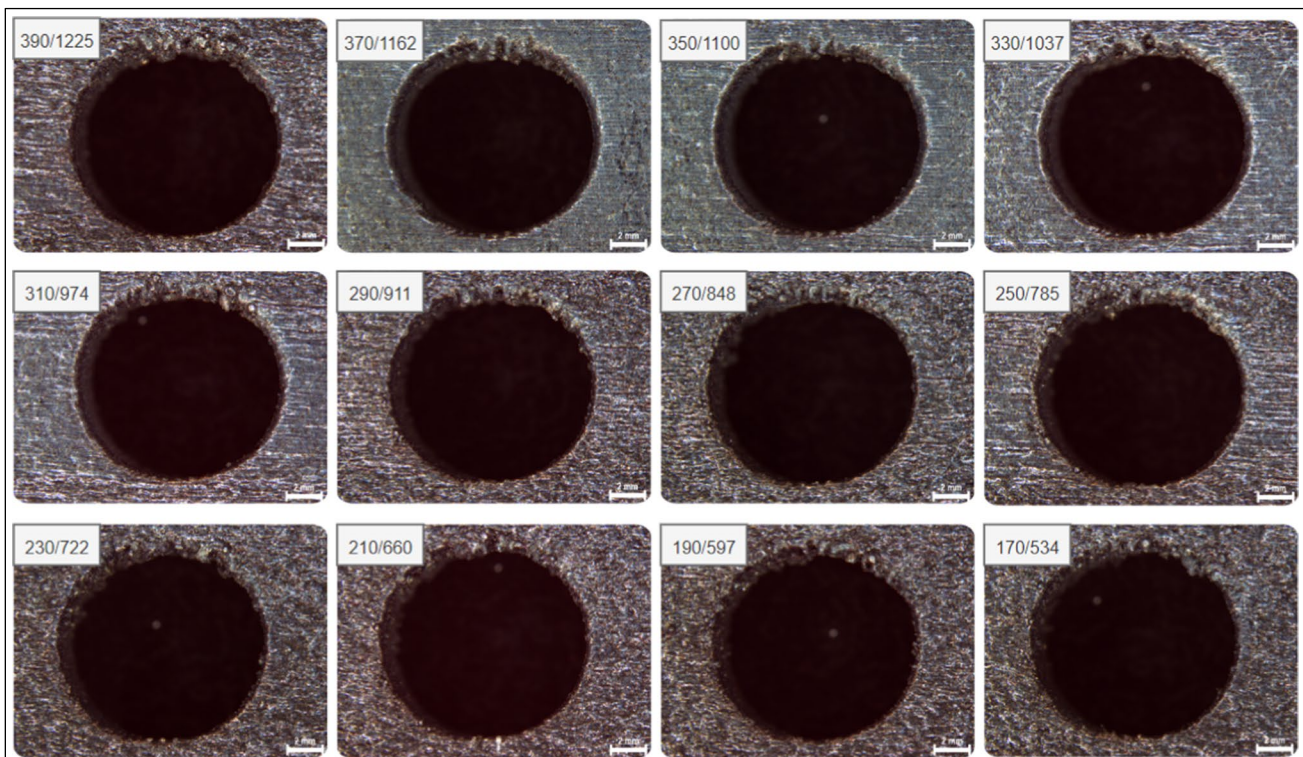
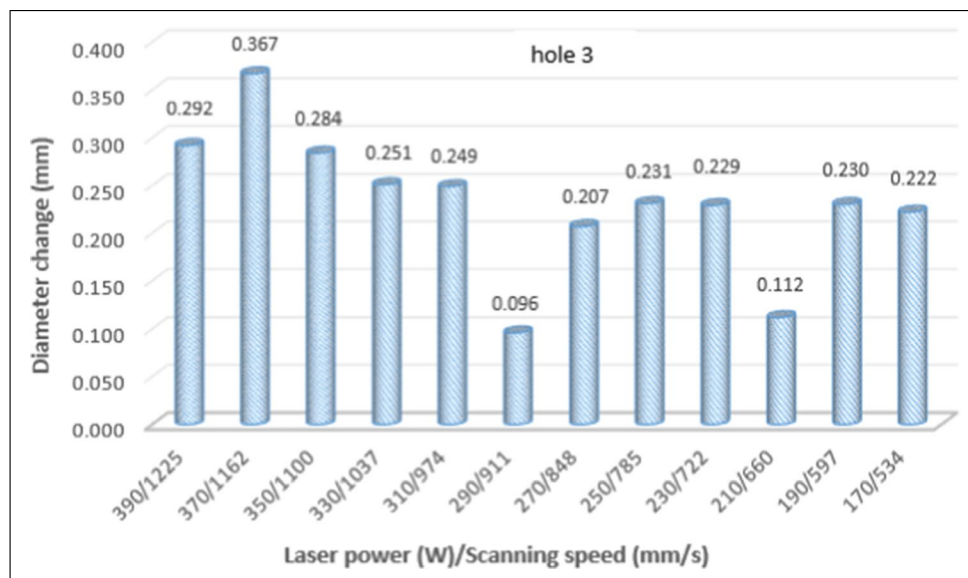
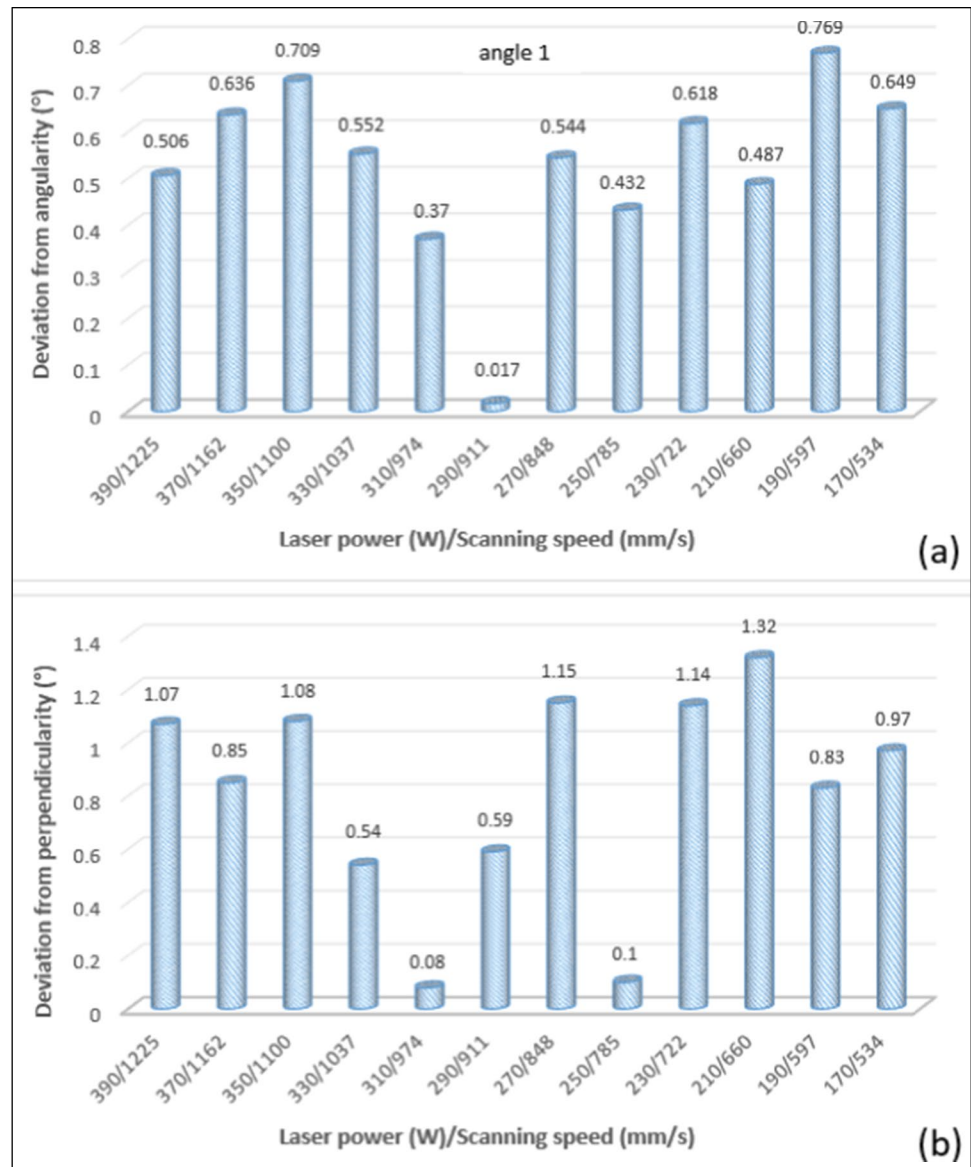


Fig. 7 Hole images taken from parts

at the 290/911 laser power/scanning speed combination. These values, like the hole diameter values, are the middle values of the manufacturing parameters. When the deviation from angularity is evaluated in terms of the specified tolerance range, angle value number 1 was obtained within the tolerance value range in part number 6. Angularity values generally result in high deviation at high and low values of

the scan power/scan speed combination. When the deviation from perpendicularity graph in Fig. 8b is examined, the lowest amount of deviation was obtained at the 310/974 laser power/scanning speed combination. When the deviation from the perpendicularity was evaluated in terms of the specified tolerance range, the desired tolerance value range was obtained in parts 5 and 8.

Fig. 8 Variation of deviation from angularity and perpendicularity according to manufacturing parameters



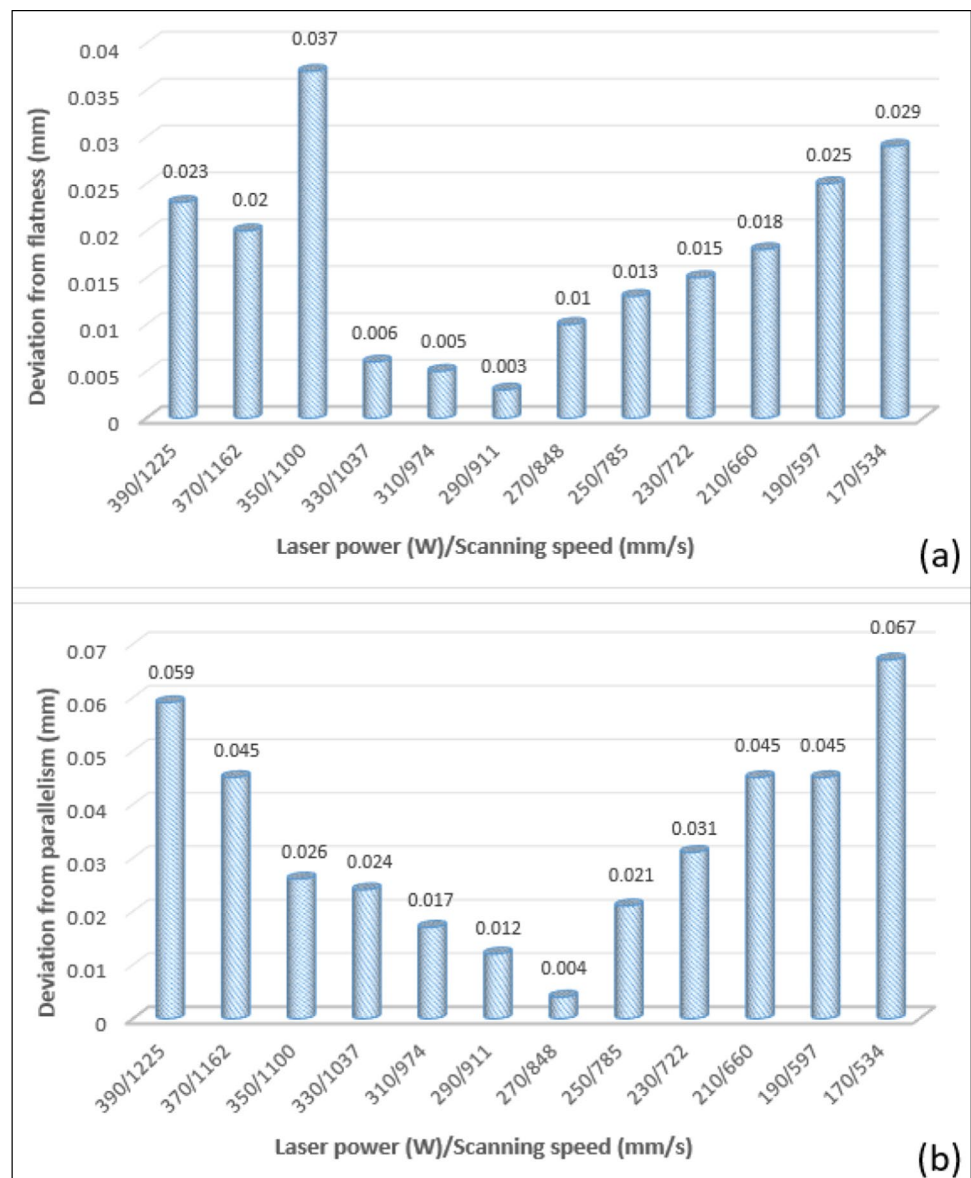
Dimensional change mainly occurs due to shrinkage due to heat energy applied during the sintering process [53]. Shrinkage causes internal stress, which affects the deformation of its parts [54]. Studies have shown that thin structures and layers are more effective on geometric accuracy, and that the production of these structures can be achieved with a smaller melting pool, and that problems in the part can be reduced by optimizing the laser parameters [55]. It has been noted that low energy input and a short scan line cause smaller residual stress in the parts [56]. In an experimental study, it was stated that as the energy input increased, higher residual stress occurred in 316-L stainless steel parts [55]. It can be said that high deviations in angularity and steepness are caused by dimensional deviations resulting from residual stresses that occur at high values of manufacturing parameters. Deviations

occurring at low values of manufacturing parameters can be explained by the formation of defects due to a lack of fusion.

3.3 Evaluation of deviation from flatness and parallelism

The variation of deviation from planarity and parallelism in additive manufacturing of AlSi10Mg alloy depending on laser power and scanning speed parameters is given in Fig. 9. When the deviation from the planarity graph given in Fig. 9a is examined, the lowest amount of deviation was obtained at the 290/911 laser power/scanning speed combination. This value is also within the middle range of manufacturing parameters that are ideal for other performance outcomes evaluated. Flatness values

Fig. 9 Variation of deviation from flatness and parallelism according to manufacturing parameters



generally increased at high and low values of the scanning power/scanning speed combination. However, it did not result in high amounts of deviation as in other performance outcomes. When the deviation from flatness was evaluated in terms of the specified tolerance range, it was found that it did not exceed the desired tolerance value in all parts, and low deviation values were obtained in all combinations of manufacturing parameters. When the deviation from the parallelism graph given in Fig. 9b is examined, the lowest amount of deviation was obtained at the 270/848 laser power/scanning speed combination. Parallelism values generally increased at high and low values of the scanning power/scanning speed combination. This tendency to deviate from parallelism exhibited similar behavior to planarity. When the deviation from parallelism was evaluated in terms of the specified

tolerance range, it was found that it did not exceed the desired tolerance value in all parts, as in the deviation from planarity values, and low deviation values were obtained in all combinations of manufacturing parameters. In metal-based additive manufacturing, surface roughness largely depends on laser processing parameters and melt pool control [57].

It has been emphasized that at very high values of laser power, excessive energy density in the melt pool causes dust spattering, which can lead to a relatively poor surface quality [58]. In addition, low surface quality is achieved by the formation of partially melted powder particles on the part surface with low energy input [59]. Deviation values from flatness and parallelism can be explained by the surface roughness that occurs at high and low values of manufacturing parameters.

Table 6 Deviation sequence, coefficients, GRG, and order values

Part no	Deviation sequence						Coefficients						GRG	Order
	DC	AD	PD	FD	PAD	DC	AD	PD	FD	PAD				
1	0.7232	0.6503	0.7984	0.5882	0.8730	0.4087	0.4347	0.3851	0.4595	0.3642	0.4104	11		
2	1.0000	0.8231	0.6210	0.5000	0.6508	0.3333	0.3779	0.4460	0.5000	0.4345	0.4183	9		
3	0.6937	0.9202	0.8065	1.0000	0.3492	0.4189	0.3521	0.3827	0.3333	0.5888	0.4152	10		
4	0.5720	0.7114	0.3710	0.0882	0.3175	0.4664	0.4127	0.5741	0.8500	0.6117	0.5830	5		
5	0.5646	0.4694	0.0000	0.0588	0.2063	0.4697	0.5158	1.0000	0.8947	0.7079	0.7176	2		
6	0.0000	0.0000	0.4113	0.0000	0.1270	1.0000	1.0000	0.5487	1.0000	0.7975	0.8692	1		
7	0.4096	0.7008	0.8629	0.2059	0.0000	0.5497	0.4164	0.3669	0.7083	1.0000	0.6083	4		
8	0.4982	0.5519	0.0161	0.2941	0.2698	0.5009	0.4753	0.9688	0.6296	0.6495	0.6448	3		
9	0.4908	0.7992	0.8548	0.3529	0.4286	0.5047	0.3849	0.3690	0.5862	0.5385	0.4766	7		
10	0.0590	0.6250	1.0000	0.4412	0.6508	0.8944	0.4444	0.3333	0.5313	0.4345	0.5276	6		
11	0.4945	1.0000	0.6048	0.6471	0.6508	0.5028	0.3333	0.4526	0.4359	0.4345	0.4318	8		
12	0.4649	0.8404	0.7177	0.7647	1.0000	0.5182	0.3730	0.4106	0.3953	0.3333	0.4061	12		

3.4 General evaluation of geometric deviations

The performance features of diameter change, deviation from angularity, deviation from perpendicularity, deviation from flatness, and deviation from parallelism have been evaluated separately in the previous sections. As a result of this evaluation, it was observed that the optimum manufacturing parameters varied among the performance features. The minimum deviation in angularity, flatness, and diameter change was achieved at the 290/911 laser power/scanning speed combination. On the other hand, deviation from parallelism occurred at 270/848 laser power/scanning speed, while deviation from perpendicularity was obtained at 310/974 laser power/scanning speed combination. Therefore, optimum manufacturing parameters need to be determined by a multi-criteria decision-making method.

3.5 Evaluating the experimental results with gray relational analysis

In this part of the study, the geometric tolerance indicator values obtained after additive manufacturing of the AISi10Mg alloy were optimized according to manufacturing parameters. Deviation values were used in the optimization process. All calculations were made using Eqs. 2–9, and the results are given in Tables 5 and 6.

As a first step, each deviation value was normalized. Since the deviation values were aimed at being low, the lower the better approach was used in the normalization process. In the next step, the gray relational coefficients (GRC) of each geometric tolerance indicator were determined, and the gray relational degrees (GRG) were calculated. The GRG value being equal to or close to 1 presents ideal operating conditions. According to GRG values, the most ideal alternative was obtained in piece number 6, with a value of 0.8692. The optimum manufacturing parameters in terms of geometric tolerances were determined as a 290/911 laser power/scanning speed combination.

4 Conclusions

In this study, the effects of laser power and scanning speed on geometric tolerances in the additive manufacturing of AISi10Mg alloy were investigated. The optimal manufacturing parameters were tried to be determined by the multi-criteria decision-making method for all geometric tolerance indicators. In this context, the gray relational analysis method was used. The results obtained in this study are given below.

- The minimum deviation in angularity, flatness, and diameter change was achieved at the 290/911 laser power/scanning speed combination. It has been observed that the deviation tends to increase at low and high values of manufacturing parameters.
- Deviation from parallelism was achieved at a minimum level at the 270/848 laser power/scanning speed combination. The amount of deviation increased with increasing and decreasing values of this combination.
- The minimum deviation in steepness was achieved at a laser power/scanning speed combination of 310/974. As with other performance features, the amount of deviation increased with decreasing and increasing values of manufacturing parameters.
- With the gray relational analysis method, the optimum manufacturing parameters for geometric tolerances were obtained as a 290/911 laser power/scanning speed combination.
- It has been revealed that laser power and scanning speed parameters are critical for product quality in the additive manufacturing of AlSi10Mg alloy.

Author contribution Yusuf Siyambaş: preparing test samples, experimental study, writing. Yakup Turgut: supervising, evaluation of results and editing.

Funding Open access funding provided by the Scientific and Technological Research Council of Türkiye (TÜBİTAK). This study was supported by Gazi University scientific research project. The authors would like to thank the University for their support. Project number: FDK-2022–7432.

Data availability The authors declare that all data obtained from the experimental study are included in this article and that the data is not used in any data repository.

Declarations

Conflict of interest The authors declare no competing interests.

Open Access This article is licensed under a Creative Commons Attribution 4.0 International License, which permits use, sharing, adaptation, distribution and reproduction in any medium or format, as long as you give appropriate credit to the original author(s) and the source, provide a link to the Creative Commons licence, and indicate if changes were made. The images or other third party material in this article are included in the article's Creative Commons licence, unless indicated otherwise in a credit line to the material. If material is not included in the article's Creative Commons licence and your intended use is not permitted by statutory regulation or exceeds the permitted use, you will need to obtain permission directly from the copyright holder. To view a copy of this licence, visit <http://creativecommons.org/licenses/by/4.0/>.

References

1. Amir B, Gale Y, Sadot A, Samuha S, Sadot O (2022) Study on the effects of manufacturing parameters on the dynamic properties of AlSi10Mg under dynamic loads using Taguchi procedure. *Mater Des* 223:111125. <https://doi.org/10.1016/j.matdes.2022.111125>
2. Dedeakayogulları H, Kacal A (2022) Experimental investigation of hole quality in drilling of additive manufacturing Ti6Al4V parts produced by hole features. *J Manuf Process* 79:745–758. <https://doi.org/10.1016/j.jmapro.2022.04.039>
3. Calignano F (2018) Investigation of the accuracy and roughness in the laser powder bed fusion process. *Virtual Phys Prototyp* 13(2):97–104. <https://doi.org/10.1080/17452759.2018.1426368>
4. Han T, Liu Y, Yang D, Qu N, Liao M, Lai Z, Zhu J (2022) Effect of annealing on microstructure and mechanical properties of AlCrFe2Ni2 medium entropy alloy fabricated by laser powder bed fusion additive manufacturing. *Mater Sci Eng A* 839:142868. <https://doi.org/10.1016/j.msea.2022.142868>
5. Jiang M, Mukherjee T, Du Y, DebRoy T (2022) Superior printed parts using history and augmented machine learning. *npj Comput Mater* 8 (1): 184. <https://doi.org/10.1038/s41524-022-00866-9>
6. Han T, Chen J, Wei Z, Qu N, Liu Y, Yang D, Zhu J (2023) Effect of cooling rate on microstructure and mechanical properties of AlCrFe2Ni2 medium entropy alloy fabricated by laser powder bed fusion. *J Market Res* 25:4063–4073. <https://doi.org/10.1016/j.jmrt.2023.06.241>
7. Hawkins AE (1993) *The shape of powder-particle outlines*. T Research Studies Press Ltd, England
8. Yalçın B, Karakılınç U, Ergene B (2019) Toz yataklı/beslemeli eklemeli imalatta kullanılan partiküllerin uygunluk araştırması ve partikül imalat yöntemleri. *Politeknik Dergisi* 22(4):801–810. <https://doi.org/10.2339/politeknik.423707>
9. Ponticelli GS, Giannini O, Guarino S, Horn M (2020) An optimal fuzzy decision-making approach for laser powder bed fusion of AlSi10Mg alloy. *J Manuf Process* 58:712–723. <https://doi.org/10.1016/j.jmapro.2020.08.054>
10. Kamarudin K, Wahab MS, Shayfull Z, Ahmed A, Raus AA (2016) Dimensional accuracy and surface roughness analysis for AlSi10Mg produced by selective laser melting (SLM). In *MATEC Web of Conferences* 78:01077. <https://doi.org/10.1051/mateconf/20167801077>
11. Wang LZ, Chen T, Wang S (2017) Microstructural characteristics and mechanical properties of carbon nanotube reinforced AlSi10Mg composites fabricated by selective laser melting. *Optik* 143:173–179. <https://doi.org/10.1016/j.jjleo.2017.06.086>
12. Read N, Wang W, Essa K, Attallah MM (2015) Selective laser melting of AlSi10Mg alloy: process optimisation and mechanical properties development. *Materials Design* 65:417–424. <https://doi.org/10.1016/j.matdes.2014.09.044>
13. Boban J, Ahmed A, Jithinraj EK, Rahman MA, Rahman M (2022) Polishing of additive manufactured metallic components: retrospect on existing methods and future prospects. *Int J Adv Manuf Technol* 121:83–125. <https://doi.org/10.1007/s00170-022-09382-y>
14. Tian Y, Tomus D, Rometsch P, Wu X (2017) Influences of processing parameters on surface roughness of Hastelloy X produced by selective laser melting. *Addit Manuf* 13:103–112. <https://doi.org/10.1016/j.addma.2016.10.010>
15. Nguyen QB, Luu DN, Nai SML, Zhu Z, Chen Z, Wei J (2018) The role of powder layer thickness on the quality of SLM printed parts. *Arch Civ Mech Eng* 18:948–955. <https://doi.org/10.1016/j.acme.2018.01.015>
16. Calignano F, Manfredi D, Ambrosio EP, Iuliano L, Fino P (2013) Influence of process parameters on surface roughness of aluminum parts produced by DMLS. *Int J Adv*

- Manufact Technol 67:2743–2751. <https://doi.org/10.1007/s00170-012-4688-9>
17. Mumtaz K, Hopkinson N (2009) Top surface and side roughness of Inconel 625 parts processed using selective laser melting. *Rapid Prototyp J* 15(2):96–103. <https://doi.org/10.1108/13552540910943397>
 18. Gruber S, Grunert C, Riede M, López E, Marquardt A, Brueckner F, Leyens C (2020) Comparison of dimensional accuracy and tolerances of powder bed based and nozzle based additive manufacturing processes. *J Laser Appl* 32(3). <https://doi.org/10.2351/7.0000115>
 19. Liu Y, Yang Y, Wang D (2017) Investigation into the shrinkage in Z-direction of components manufactured by selective laser melting (SLM). *The Int J Adv Manuf Technol* 90:2913–2923. <https://doi.org/10.1007/s00170-016-9596-y>
 20. Pant M, Nagdeve L, Moona G, Kumar H (2022) Estimation of measurement uncertainty of additive manufacturing parts to investigate the influence of process variables. *Mapan* 37(4):765–775. <https://doi.org/10.1007/s12647-022-00592-z>
 21. Zhang L, Zhang S, Zhu H, Hu Z, Wang G, Zeng X (2018) Horizontal dimensional accuracy prediction of selective laser melting. *Mater Des* 160:9–20. <https://doi.org/10.1016/j.matdes.2018.08.059>
 22. Han J, Wu M, Ge Y (2019) A study on the dimension accuracy on the inner structure of the 3D printed parts caused by the scanning strategy. *Materials* 12(8):1333. <https://doi.org/10.3390/ma12081333>
 23. Kayacan Y (2020) Investigation of the effect of geometric parameters on temperature distribution, residual stress and deformation in manufacturing with selective laser melting. Dissertation, University of Isparta
 24. Maamoun AH, Xue YF, Elbestawi MA, Veldhuis SC (2018) Effect of selective laser melting process parameters on the quality of al alloy parts: powder characterization, density, surface roughness, and dimensional accuracy. *Materials* 11(12):2343. <https://doi.org/10.3390/ma11122343>
 25. Lee SJ, Sachs E, Cima M (1995) Layer position accuracy in powder-based rapid prototyping. *Rapid Prototyp J* 1(4):24–37. <https://doi.org/10.1108/13552549510104447>
 26. Dsouza A (2016) Experimental evolutionary optimization of geometric integrity in Fused Filament Fabrication (FFF) Additive Manufacturing (AM) process. Dissertation, State University of New York at Binghamton
 27. Chen J, Zhang Z, Chen X, Zhang C, Zhang G, Xu Z (2014) Design and manufacture of customized dental implants by using reverse engineering and selective laser melting technology. *J Prosthet Dent* 112(5):1088–1095. <https://doi.org/10.1016/j.prosdent.2014.04.026>
 28. Juechter V, Franke MM, Merenda T, Stich A, Körner C, Singer RF (2018) Additive manufacturing of Ti-45Al-4Nb-C by selective electron beam melting for automotive applications. *Addit Manuf* 22:118–126. <https://doi.org/10.1016/j.addma.2018.05.008>
 29. Minetola P, Galati M, Calignano F, Iuliano L, Rizza G, Fontana L (2020) Comparison of dimensional tolerance grades for metal AM processes. *Procedia CIRP* 88:399–404. <https://doi.org/10.1016/j.procir.2020.05.069>
 30. Franchitti S, Borrelli R, Pirozzi C, Carrino L, Polini W, Sorrentino L, Gaggero A (2018) Investigation on Electron Beam Melting: dimensional accuracy and process repeatability. *Vacuum* 157:340–348. <https://doi.org/10.1016/j.vacuum.2018.09.007>
 31. Toguem SCT, Rupal BS, Mehdi-Souzani C, Qureshi AJ, Anwer N (2018) A review of AM artifact design methods. In: *Proceedings-2018 ASPE uspen summer topical meeting: advancing precision in additive manufacturing*, pp 132–137
 32. Toguem SCT, Mehdi-Souzani C, Noura H, Anwer N (2020) Axiomatic design of customised additive manufacturing artefacts. *Procedia CIRP* 91:899–904. <https://doi.org/10.1016/j.procir.2020.02.246>
 33. Moylan S, Slotwinski J, Cooke A, Jurens K, Donmez MA (2012) Proposal for a standardized test artifact for additive manufacturing machines and processes. <https://doi.org/10.26153/tsw/15399>
 34. Mahesh M, Wong YS, Fuh JYH, Loh HT (2004) Benchmarking for comparative evaluation of RP systems and processes. *Rapid Prototyping Journal* 10(2):123–135. <https://doi.org/10.1108/13552540410526999>
 35. Shahrain M, Didier T, Lim GK, Qureshi AJ (2016) Fast deviation simulation for ‘fused deposition modeling’ process. *Procedia Cirp* 43:327–332. <https://doi.org/10.1016/j.procir.2016.02.004>
 36. Mahmood S, Qureshi AJ, Goh KL, Talamona D (2017) Tensile strength of partially filled FFF printed parts: experimental results. *Rapid prototyping journal* 23(1):122–128. <https://doi.org/10.1108/RPJ-08-2015-0115>
 37. Rupal BS, Anwer N, Secanell M, Qureshi AJ (2020) Geometric tolerance and manufacturing assemblability estimation of metal additive manufacturing (AM) processes. *Mater Des* 194:108842. <https://doi.org/10.1016/j.matdes.2020.108842>
 38. Mahmood S, Qureshi AJ, Talamona D (2018) Taguchi based process optimization for dimension and tolerance control for fused deposition modelling. *Addit Manuf* 21:183–190. <https://doi.org/10.1016/j.addma.2018.03.009>
 39. Akdulum A, Kayir Y (2023) Experimental investigation and optimization of process stability in drilling of Al 7075–T651 using indexable insert drills. *J Braz Soc Mech Sci Eng* 45(8):429. <https://doi.org/10.1007/s40430-023-04303-w>
 40. Abdallah S, Ali S, Pervaiz S (2023) Performance optimization of 3D printed polyamide 12 via Multi Jet Fusion: a Taguchi grey relational analysis (TGRA). *Int J Light Mater Manuf* 6(1):72–81. <https://doi.org/10.1016/j.ijlmm.2022.05.004>
 41. Çakıroğlu R, Günay M (2020) Comprehensive analysis of material removal rate, tool wear and surface roughness in electrical discharge turning of L2 tool steel. *J Market Res* 9(4):7305–7731. <https://doi.org/10.1016/j.jmrt.2020.04.060>
 42. Ekici E, Uzun G (2022) Effects on machinability of cryogenic treatment applied to carbide tools in the milling of Ti6Al4V with optimization via the Taguchi method and grey relational analysis. *J Braz Soc Mech Sci Eng* 44(7):270. <https://doi.org/10.1007/s40430-022-03572-1>
 43. Siyambaş Y, Turgut Y (2023) Experimental and statistical investigation of mechanical properties and surface roughness in additive manufacturing with selective laser melting of AlSi10Mg alloy. *J Braz Soc Mech Sci Eng* 45(10):515. <https://doi.org/10.1007/s40430-023-04445-x>
 44. Kladovasilakis N, Charalampous P, Kostavelis I, Tzetzis D, Tzovaras D (2021) Impact of metal additive manufacturing parameters on the powder bed fusion and direct energy deposition processes: A comprehensive review. *Progr Add Manuf* 6:349–365. <https://doi.org/10.1007/s40964-021-00180-8>
 45. A P, CI AP, C (2021) AlSi10 Mg powder data sheet. https://www.htitjo.com/product_details/10.html
 46. ASME Y14.5-2009 (2009) Dimensioning and tolerancing. ASME, New York. <https://tajhizkala.ir/doc/ASME/ASME%20Y14.5-2009-03.pdf>
 47. Haq AN, Marimuthu P, Jeyapaul R (2008) Multi response optimization of machining parameters of drilling Al/SiC metal matrix composite using grey relational analysis in the Taguchi method. *Int J Adv Manuf Technol* 37:250–255. <https://doi.org/10.1007/s00170-007-0981-4>
 48. Palanikumar K (2011) Experimental investigation and optimisation in drilling of GFRP composites. *Measurement* 44(10):2138–2148. <https://doi.org/10.1016/j.measurement.2011.07.023>
 49. Taşkesen A, Küçük K (2014) Experimental investigation and multi-objective analysis on drilling of boron carbide reinforced

- metal matrix composites using grey relational analysis. *Measurement* 47:321–330. <https://doi.org/10.1016/j.measurement.2013.08.040>
50. Fu C, Zheng J, Zhao J, Xu W (2001) Application of grey relational analysis for corrosion failure of oil tubes. *Corros Sci* 43(5):881–889. [https://doi.org/10.1016/S0010-938X\(00\)00089-5](https://doi.org/10.1016/S0010-938X(00)00089-5)
51. Murr LE, Gaytan SM, Ramirez DA, Martinez E, Hernandez J, Amato KN, Wicker RB (2012) Metal fabrication by additive manufacturing using laser and electron beam melting technologies. *J Mater Sci Technol* 28(1):1–14. [https://doi.org/10.1016/S1005-0302\(12\)60016-4](https://doi.org/10.1016/S1005-0302(12)60016-4)
52. Charles A, Elkaseer A, Thijs L, Hagemeyer V, Scholz S (2019) Effect of process parameters on the generated surface roughness of down-facing surfaces in selective laser melting. *Appl Sci* 9(6):1256. <https://doi.org/10.3390/app9061256>
53. Zheng H, Zhang J, Lu S, Wang G, Xu Z (2006) Effect of core-shell composite particles on the sintering behavior and properties of nano-Al₂O₃/polystyrene composite prepared by SLS. *Mater Lett* 60(9–10):1219–1223. <https://doi.org/10.1016/j.matlet.2005.11.003>
54. Pradeep AD, Rameshkumar T, Kumar M (2021) Parameter optimization of SLS Sinterstation 2500plus using GRA for better surface finish and dimensional accuracy. *Mater Today: Proceed* 45:8105–8109. <https://doi.org/10.1016/j.matpr.2021.01.638>
55. Bartlett JL, Li X (2019) An overview of residual stresses in metal powder bed fusion. *Addit Manuf* 27:131–149. <https://doi.org/10.1016/j.addma.2019.02.020>
56. Liu Y, Yang Y, Wang D (2016) A study on the residual stress during selective laser melting (SLM) of metallic powder. *Int J Adv Manuf Technol* 87:647–656. <https://doi.org/10.1007/s00170-016-8466-y>
57. Mumtaz KA, Hopkinson N (2010) Selective laser melting of thin wall parts using pulse shaping. *J Mater Process Technol* 210(2):279–287. <https://doi.org/10.1016/j.jmatprotec.2009.09.011>
58. Brecher C, Jeschke S, Schuh, Aghassi, S, Arnoscht J, Bauhoff F, ... Jeschke S (2011) Integrative production technology for high-wage countries. In *Integrative production technology for high-wage countries* 17–76
59. Wang LZ, Wang S, Wu JJ (2017) Experimental investigation on densification behavior and surface roughness of AlSi10Mg powders produced by selective laser melting. *Opt Laser Technol* 96:88–96. <https://doi.org/10.1016/j.optlastec.2017.05.006>

Publisher's Note Springer Nature remains neutral with regard to jurisdictional claims in published maps and institutional affiliations.